

Spherical accretion in the Schwarzschild spacetime in the Newtonian analogous construct

SHUBHRANGSHU GHOSH,^{1,2} SOUVIK GHOSE,³ KALYANBRATA PAL,³ ARUNABHA BHADRA,⁴ AND TAPAS K. DAS^{3,5}

¹*Center for Astrophysics, Gravitation and Cosmology, Shri Ramasamy Memorial (SRM) University Sikkim,
5th Mile Tadong, Gangtok, 737102, India*

²*Department of Physics, Shri Ramasamy Memorial (SRM) University Sikkim, 5th Mile Tadong, Gangtok, 737102, India*

³*Harish-Chandra Research Institute, HBNI, Chhatnag Road, Jhansi, Allahabad, 211109, India*

⁴*High Energy & Cosmic Ray Research Centre, University of North Bengal, Siliguri, 734013, India*

⁵*Physics and Applied Mathematics Unit, Indian Statistical Institute, 203 Barrackpore Trunk Road, Kolkata, 700108, India*

ABSTRACT

The velocity-dependent Newtonian analogous potentials (NAPs) corresponding to general relativistic (GR) spacetimes accurately capture most of the relativistic features, including all classical tests of GR, effectively representing spacetime geometries in Newtonian terms. The NAP formulated by Tejada & Rosswog (TR13) for Schwarzschild spacetime has been applied to the standard thin accretion disk around a black hole (BH) as well as in the context of streamlines of noninteracting particles accreting onto a Schwarzschild BH, showing good agreement with the exact relativistic solutions. As a further application, here we explore the extent to which TR13 NAP could describe a transonic hydrodynamical spherical accretion flow in Schwarzschild spacetime within the framework of standard Newtonian hydrodynamics. Instead of obtaining a typical single “saddle-type” sonic transition, a “saddle–spiral pair” is produced, with the inner sonic point being an (unphysical) “spiral type” and the outer being a usual “saddle type.” The Bondi accretion rate at outer sonic radii, however, remains consistent with that of the GR case. The primary reason for the deviation of our findings from the classical Bondi solution is likely due to the inconsistency between the Euler-type equation in the presence of velocity-dependent TR13 NAP within the standard Newtonian hydrodynamics framework, and the corresponding GR Euler equation, regardless of the fluid’s energy. Our study suggests that a (modified) hydrodynamical formalism is needed to effectively implement such potentials in transonic accretion studies that align with the spirit of TR13 like NAP, while remaining consistent with the GR hydrodynamics. This could then essentially circumvent GR hydrodynamics or GR magnetohydrodynamics equations

Keywords: accretion, accretion disks — black hole physics — hydrodynamics — gravitation — relativistic processes

1. INTRODUCTION

shubhrangshughosh.r@srmus.edu.in

souvikghose@hri.res.in

kalyanbratopal@hri.res.in

aru_bhadra@yahoo.com

tapas@hri.res.in

Corresponding author: Tapas K. Das
tapas@hri.res.in

In recent times, Newtonian-like analogous potentials (hereinafter NAPs) of corresponding general relativistic (GR) spacetime geometries have been constructed in the literature (Tejeda & Rosswog (2013), hereinafter TR13; Ghosh et al. (2014, 2015); Sarkar et al. (2014); Ghosh et al. (2016)), with an intent to have an accurate or correct representation of spacetime geometries (or metric theories of gravity) in the Newtonian framework. Following TR13, most of these NAPs have been derived from the Hamiltonian of the test particle motion, starting from the actual geodesic motion of test particles in corresponding spacetimes (TR13; Ghosh et al. (2014, 2015); Sarkar et al. (2014)). The analogous potentials comprise of the terms containing explicit information of the velocity of the particle motion, in addition to the spherically symmetric part of the gravitational source and the other source specific terms.

In the far (weak) field gravity at (nearly) static conditions, spherically symmetric Newtonian gravitational potential continues to be used in almost all applications as a valid approximation, however, its description fails to account for most of the effects in strong field gravity, even approximately. Previously, efforts have been undertaken to modify the Newtonian potential by tweaking its form to mathematically replicate or mimic certain GR features of corresponding spacetime geometries, primarily to describe the inner relativistic accretion flow dynamics in the vicinity of black holes (BHs)/compact objects. These modified potentials are commonly referred to as pseudo-Newtonian potentials (PNPs). Several such PNPs have been introduced in the literature soon after its inception by Paczynsky & Wiita (1980) (hereinafter PW80) to reproduce certain relativistic features of Schwarzschild BH, either through ad hoc proposition or following certain specific methods (see for e.g., Mukhopadhyay (2002); Ghosh & Mukhopadhyay (2007)). For an elaborate discussion regarding various aspects of PNPs, see for e.g., TR13; Ghosh et al. (2016); Witzany & Lämmerzahl (2017) and references in them. While prescribing the PNPs, the emphasis are mostly laid to correctly reproduce the innermost stable and bound circular orbits, without endeavoring to actually construct any Newtonian analogues of corresponding spacetime geometries. PNPs, thus, lack the uniqueness to describe the dynamical properties of corresponding spacetimes in its entirety, within a reasonable accuracy.

As the effect of a spacetime geometry could only be perceived through the dynamics of geodesic motion, any correct analogous construct of metric theory of gravity in the Newtonian framework should then explicitly contain the information of the velocity of the particle motion. In this context, more recently, adhering to a first-principle approach, Ghosh et al. (2016) formulated an exact relativistic Newtonian analogue of spherically symmetric static spacetime metrics, described through a relativistic gravitational action in the Newtonian picture, furnishing identical geodesic equations of motion to those of the parent metric. The corresponding velocity-dependent NAP exactly reproduces all relativistic gravitational features of corresponding spacetime geometry for a distant stationary observer, including all the existing classical tests of GR. In general, velocity-dependent NAPs are far more accurate representations of relativistic spacetime geometries in analogous Newtonian framework, with an ability to uniquely describe the corresponding spacetime dynamics more precisely (for more details, see the references in the first paragraph of this section). For more comments on velocity dependent NAPs and their interpretation, readers can follow Witzany & Lämmerzahl (2017); Friedman & Scarr (2019); Friedman et al. (2019).

One of the potential astrophysical scenarios where modified Newtonian-like potential could be useful is the relativistic accretion phenomena around BHs/compact objects. In this regard, the existing PNPs, particularly PW80 or for that matter, Mukhopadhyay (2002) or Ghosh & Mukhopadhyay (2007) potentials had been used quite extensively in the astrophysical literature, to study the complex inner accretion flow dynamics around non-rotating/rotating BHs (e.g., Matsumoto et al. (1984); Abramowicz et al. (1988); Chakrabarti & Titarchuk (1995); Chakrabarti (1996); Hawley & Krolik (2002); Hawley & Balbus (2002); Igumenshchev et al. (2003); Chan et al. (2005); Lipunov & Gorbovskoy (2007); Igumenshchev (2008); Shafee et al. (2008); Benson & Babul (2009); Bhattacharya et al. (2010); Ohsuga & Mineshige (2011); Narayan & Fabian (2011); Yuan & Narayan (2014) and references therein; Bu et al. (2016); Mondal & Mukhopadhyay (2019); Dihingia et al. (2020)) The approximation scheme through which the PNPs are implemented is by simply replacing the Newtonian gravitational potential (or force) by these modified potentials in the Newtonian hydrodynamical equations. As velocity-dependent NAPs are more accurate representations of corresponding spacetime metrics, it would be then worthwhile to investigate, how far one can make use of this formalism in hydrodynamical accretion studies within the framework of standard Newtonian hydrodynamics. The NAP developed by TR13 under the low-energy limit condition, for Schwarzschild spacetime, which can accurately capture most of all the corresponding relativistic features of Schwarzschild spacetime, including the classical experimental tests of GR, has been applied to the standard geometrically thin accretion disk, and is found to be in good agreement with the relativistic value of radiative energy flux emitted from the disk. In addition, the said NAP can reproduce the relativistic streamlines of non-interacting particles accreting onto a Schwarzschild BH (Tejeda et al. (2012, 2013); TR13). Bonnerot et al. (2016)

have recently used the velocity-dependent analogous potential of TR13 effectively, in the context of tidal disruption of stars by Schwarzschild BHs, within the framework of smooth particle hydrodynamics (SPH).

As a further astrophysical application, we, here, explore the extent to which TR13 NAP could describe a transonic radial/quasi-radial type (hydrodynamical) accretion flow in Schwarzschild spacetime, i.e., a Bondi-type hydrodynamical spherical accretion Bondi (1952) within the framework of standard Newtonian hydrodynamics, by performing an actual hydrodynamical study. Extensive investigations on Bondi-type spherical flows have been undertaken by several authors to address the critical properties of such flows, and have been revisited time and again from multiple angles in both GR as well as in pseudo-GR regimes (e.g., Michel (1972); Flammang (1982); Turolla & Nobili (1989); Chang & Ostriker (1985); Nobili & Turolla (1988); Nobili et al. (1991); Das & Sarker (2001); Das (2002a); Mandal et al. (2007); Ghosh & Banik (2015); Korol et al. (2016); Ciotti & Pellegrini (2017); Ramírez-Velasquez et al. (2018); Raychaudhuri et al. (2018, 2021); Ramírez-Velasquez et al. (2019); Richards et al. (2021); Yang et al. (2021); Aguayo-Ortiz et al. (2021); Mancino et al. (2022)). Recently, few authors have also investigated such Bondi-type spherical accretion in modified Einsteinian gravities (e.g., John & Stevens (2019); Kalita & Mukhopadhyay (2019); Bauer et al. (2022)). Classical Bondi flow onto a point gravitating mass exhibits transonic behavior, usually described by a single (saddle-type) critical transition. However, instances of violation of this ‘‘criticality-condition’’ or appearance of multi-critical points in spherical accretion has been addressed by several authors in the literature (e.g., Flammang (1982); Turolla & Nobili (1988, 1989); Nobili et al. (1991); Mandal et al. (2007); Ghosh & Banik (2015); Raychaudhuri et al. (2018, 2021)). Mandal et al. (2007), in fact, discussed the possibility of having three critical points in the spherical accretion flow onto a Schwarzschild BH in the GR framework, through dynamical systems analysis ¹.

The rest of the paper is as follows: In the next section we will formulate our hydrodynamical model for Bondi-type spherical accretion in the presence of the analogous potential of TR13, and perform the global critical point analysis in the parameter space. In §3 we investigate the nature of critical points from dynamical system analysis. §4 deals with the fluid behavior of spherical type flows in the presence of such velocity-dependent potential and flow topology for such a system. Finally, we culminate in §5 with a discussion and general remarks on our findings.

2. HYDRODYNAMICAL FORMALISM OF SPHERICAL ACCRETION FLOW IN THE PRESENCE OF VELOCITY-DEPENDENT ANALOGOUS POTENTIAL AND GLOBAL CRITICAL POINT ANALYSIS

Preserving the conventional approach, we consider a quasi-stationary spherically symmetric accretion flow onto a Schwarzschild BH. Consequently, we assume the flow to be inviscid in nature. Here it is to be noted that although ‘ $r\phi$ ’ component of viscous stress tensor is discarded owing to the consideration of spherical flow, however, ‘ rr ’ component of the stress tensor might not altogether be neglected. Nonetheless, following the arguments in Narayan & Fabian (2011) and Raychaudhuri et al. (2018), we discard the above stated stress tensor term in our present work. It would be interesting to investigate the effect of this term on the Bondi solution, which however, is beyond the scope of the present work, and left for future analysis. As the flow is inviscid, we further neglect the heat generation and radiative loss from the system. Being spherically symmetric, we express the dynamical flow variables only as functions of radius r . Throughout our analysis, r is expressed in units of $r_g = GM_{\text{BH}}/c^2$, where M_{BH} is the BH mass, c the speed of light, and G the usual gravitational constant. Radial velocity v and sound speed c_s are expressed in units of c . The accretion flow is considered to be polytropic with equation of state given by $P = K\rho^{1+1/n}$, where P and ρ are the usual gas pressure and density of the accreting plasma. K is a constant which contains the information of the entropy content of the flow. The polytropic index n is related to the adiabatic index γ through the usual relation $n = \frac{1}{\gamma-1}$, where γ varies between $4/3$ and $5/3$, corresponding to relativistic and non-relativistic flows, respectively. The sound speed is given through the relation $c_s^2 = (1 + 1/n)P/\rho$. For our study, we vary the entire range of adiabatic index gamma from $4/3$ to $5/3$.

Before proceeding further, let us focus on the velocity-dependent NAP given in TR13. In dimensionless unit, the corresponding generalized potential in Boyer-Lindquist coordinate system is given by

$$\Phi_{\text{NAP}}(r, \dot{r}, \dot{\omega}) = -\frac{1}{r} - \frac{2}{r-2} \left[\left(\frac{r-1}{r-2} \right) \dot{r}^2 + \frac{r^2 \dot{\omega}^2}{2} \right], \quad (1)$$

¹ For more details on the astrophysical relevance of Bondi-type spherical accretion, readers can follow Raychaudhuri et al. (2018, 2021), and references therein

where, subscript NAP denotes Newtonian analogous potential, and $\dot{\Omega}^2 = \dot{\theta}^2 + \sin^2 \theta \dot{\phi}^2$. The potential is a reduced form of Ghosh et al. (2016) potential in the low energy limit of particle motion. As we are primarily interested in spherical-type flow, neglecting the angular part of the above expression, Eqn. (1) reduces to

$$\Phi_{\text{NAP}}(r, \dot{r}) = -\frac{1}{r} - \frac{2(r-1)\dot{r}^2}{(r-2)^2}. \quad (2)$$

One can now compute the corresponding generalized force using the relation $\mathcal{F}_{\text{NAP}} = -\frac{\partial \Phi_{\text{NAP}}}{\partial r} + \frac{d}{dt} \frac{\partial \Phi_{\text{NAP}}}{\partial \dot{r}}$, which leads to

$$\mathcal{F}_{\text{NAP}}(r, \dot{r}) = -\frac{1}{r^2} + \frac{4(r-1)}{r^4} + \frac{2\dot{r}^2}{r(r-2)}. \quad (3)$$

The above expression is identical to the expression given by Eqn. (2.14) in TR13 for purely radial motion.

Preserving the similar scheme of using existing PNP's in Newtonian hydrodynamical framework, the basic conservation equations for a stationary, inviscid spherical accretion flow in the presence of velocity-dependent force F_{NAP} given in Eqn. (3) are as follows:

(i) Baryon conservation equation:

$$\frac{d}{dr} (4\pi r^2 \rho v) = 0, \quad (4)$$

(ii) Radial momentum transfer equation:

$$v \frac{dv}{dr} + \frac{1}{\rho} \frac{dP}{dr} + \frac{1}{r^2} - \frac{4(r-1)}{r^4} - \frac{2}{r(r-2)} v^2 = 0 \quad (5)$$

Here it is to be noted that as a standard practice, in the context of fluid equations, we have identified \dot{r} as the radial velocity 'v' of the flow. Integrating Eqn. (4), one obtains the Baryon mass accretion rate \dot{M} given by $\dot{M} = -4\pi r^2 \rho v$. Combining Eqns. (4) and (5) and rearranging, we obtain

$$\frac{dv^2}{dr} = \frac{2 \left[\frac{2c_s^2}{r} - \frac{1}{r^2} + \frac{4(r-1)}{r^4} + \frac{2v^2}{r(r-2)} \right]}{1 - \frac{c_s^2}{v^2}} = \frac{N1(v, c_s, r)}{D(v, c_s)} \quad (6)$$

and

$$\frac{dc_s^2}{dr} = -\frac{1}{n} \frac{c_s^2}{v^2} \left[\frac{2v^2}{r} - \frac{1}{r^2} + \frac{4(r-1)}{r^4} + \frac{2v^2}{r(r-2)} \right] = \frac{N2(v, c_s, r)}{D(v, c_s)}, \quad (7)$$

respectively, where we identified ' $N1(v, c_s, r)$ ', ' $N2(v, c_s, r)$ ' and ' $D(v, c_s)$ ' as numerators and the denominator, respectively. The dynamics of the accretion flow is described through the Eqns. (6) and (7). Following the previous authors as before (e.g., Matsumoto et al. (1984); Fukue (1987); Chakrabarti (1989, 1990, 1996); Lu et al. (1997); Das (2002b); Mukhopadhyay & Ghosh (2003); Raychaudhuri et al. (2018, 2021)), we solve the stated equations employing the standard practice of sonic point analysis. As usual for transonic flows, a smooth and a continuous solution inevitably entails that the following identity $N1 = N2 = D = 0$ must be satisfied at a specific radial location, termed as 'critical radius' which in our case is the 'sonic radius' (r_c). At r_c , the above identity renders

$$v^2|_{r_c} = c_s^2|_{r_c} = \frac{1}{2r_c} \frac{(1 - 2/r_c)^3}{(1 - 1/r_c)} \quad (8)$$

At sonic location r_c , we apply l'Hospital's rule to respective Eqns. (6) and (7), that yields

$$\left. \frac{dv^2}{dr} \right|_{r_c} = \frac{-\mathcal{B} \pm \sqrt{\mathcal{B}^2 - 4\mathcal{A}\mathcal{C}}}{2\mathcal{A}} \quad (9)$$

and

$$\left. \frac{dc_s^2}{dr} \right|_{r_c} = -\frac{1}{N} \left[\mathcal{F}_c + \frac{1}{2} \left. \frac{dv^2}{dr} \right|_{r_c} \right], \quad (10)$$

respectively, where

$$\left. \begin{aligned} \mathcal{A} &= \frac{1}{2} (2n + 1)/n, \\ \mathcal{B} &= \frac{1}{n} \left(\frac{2v_c^2}{r_c} + \mathcal{F}_c \right) - \frac{4v_c^2}{r_c(r_c-2)}, \\ \mathcal{C} &= 2u_c^2 \left[\frac{2c_{sc}^2}{r_c^2} + \frac{2\mathcal{F}_c}{nr_c} + \left(-\frac{2}{r_c^3} - \frac{4(4-3r_c)}{r_c^5} + \frac{4(r_c-1)}{r_c^2(r_c-2)^2} \right) \right], \end{aligned} \right\} \quad (11)$$

with $\mathcal{F}_c = \frac{1}{r_c^4} \frac{(r_c-2)^3}{(r_c-1)}$. In Eqn. (9), ‘-’ sign in the ‘ \pm ’ indicates accretion solution, and the ‘+’ sign indicates the wind solution.

To understand the transonic behavior of the flow, it is necessary for us to compute ‘sonic energy’ and ‘sonic entropy’ and analyze their variation with sonic radius. Usually for non dissipative (inviscid) spherical accretion flow, specific energy of the flow is obtained by simply integrating Euler’s equation. For which case the energy remains conserved throughout the accretion flow regime, and the sonic energy (\mathcal{E}_c) is then equivalent to energy at outer accretion boundary. For our case, however, the velocity-dependent potential (or force) given in Eqn. (2) [or in Eqn. (3)] is not a conserved quantity, and consequently, the energy of the flow will not remain conserved at all radii. Nonetheless, following the standard practice used for dissipative accreting system (e.g., [Chakrabarti \(1990, 1996\)](#)), one can define the specific energy at sonic location ‘ \mathcal{E}_c ’, which for our case is given by

$$\mathcal{E}_c = \text{K.E}|_{r_c} + \text{T.E}|_{r_c} + \Phi_{\text{NAP}}(r, \dot{r})|_{r_c} - \dot{r} \left. \frac{d\Phi_{\text{NAP}}}{d\dot{r}} \right|_{r_c}, \quad (12)$$

where T.E is the thermal energy. Identifying \dot{r} as v , the expression for specific energy at r_c then follows

$$\mathcal{E}_c = \frac{1}{2} v_c^2 + n c_{sc}^2 - \frac{1}{r_c} + \frac{2(r_c-1)}{(r_c-2)^2} v_c^2. \quad (13)$$

Note that, an appropriate value of \mathcal{E}_c needs to be provided to solve the dynamical equations, as a boundary condition for the flow. Using the expressions for v_c and c_{sc} , and rearranging Eqn. (13), one obtains a polynomial equation in r_c , given by

$$2\mathcal{E}_c r_c^4 - [2\mathcal{E}_c + n - 3/2] r_c^3 - (1 - 6n) r_c^2 + 12n r_c - 8n = 0. \quad (14)$$

The specific entropy of the flow is expressed through the relation $\dot{\mu} = (\gamma K)^n |\dot{M}|$ (e.g., [Chakrabarti \(1989, 1990, 1996\)](#); [Raychaudhuri et al. \(2018, 2021\)](#)). At sonic location, the expression for sonic entropy is given by

$$\dot{\mu}_c = 4\pi r_c^2 \left[\frac{(r_c-2)^3}{2r_c^3 (r_c-1)} \right]^{(2n+1)/2}. \quad (15)$$

Classical Bondi-type accretion onto a point gravitating source is a transonic flow usually characterized by a single ‘saddle-type’ sonic point; the physically meaningful critical point through which the physical accretion flow passes continuously connecting infinity to BH event horizon, entering the BH supersonically. However, it would be interesting

to check, whether such ‘*criticality-condition*’ would remain intact or gets violated in the fluid flow, for our scenario. Here, we examine the transonic behavior of adiabatic class of such spherical Bondi-type flows in the presence of velocity-dependent potential [as described in Eqn. (2)] in the standard Newtonian hydrodynamical framework we adopted here. One can determine the transonic behavior of fluid flows from Eqn. (14) and/or Eqn. (15), through $\mathcal{E}_c - r_c$, and/or $\dot{\mu}_c - r_c$ profiles, respectively.

Figures 1(a),(b),(c) depict the variation of \mathcal{E}_c as a function of r_c corresponding to different values of adiabatic constant γ . The profiles indicate a departure of the flow from the that of classical Bondi solution, with the likely emergence of *two sonic points* (or two critical points) in the flow at all radii outside the horizon. Let us now focus on any one of the $\mathcal{E}_c - r_c$ profiles. The outer sonic points having negative slopes of the curve are all likely to be ‘saddle-type’ or ‘X-type’ sonic points through which the flow attains supersonic speed. Conversely, the inner sonic point branch having the positive slope does not likely to be consisting of ‘saddle-types’, rather ‘centre-types’ (‘O-types’) or ‘spiral-types’. Nonetheless, the outer sonic points almost coincide with that of the sonic locations corresponding to classical Bondi case. Even though, in two sonic-point scenario, had both the sonic points being ‘saddle-types’, it would not have been possible to connect two sonic points through continuous solutions (e.g., Mandal et al. (2007)). On the other hand, in the context of well-behaved fixed points, it has been pointed out before that two adjacent fixed points can never be both ‘saddle-types’ (Jordan & Smith 2007)

In Figs 1(d),(e),(f) we depict the variation of \mathcal{E}_c as a function of $\dot{\mu}_c$. The profiles show that the curves do not (or tend to) form closed loops, as is being expected from the analysis of $\mathcal{E}_c - r_c$ profiles. The upper portion branch of the curves plausibly indicate outer ‘X-type’ sonic point branch. Had thee sonic points emerged in our flow, the curves would have formed closed loops with the likely appearance of inner ‘X-type’ sonic point branch in $\mathcal{E}_c - \dot{\mu}_c$ profiles (namely, ‘swallowtail catastrophe’, see for e.g., Chakrabarti (1989, 1990)).

To understand the flow behavior, one needs a robust and thorough analysis about the nature of the critical points, which we pursue in the following section.

3. PROPERTIES OF THE CRITICAL POINTS

Following, for e.g., Mandal et al. (2007); Kato & Fukue (2020)(hereinafter KF20); Yang et al. (2021), and references in them, one can represent the steady, spherically symmetric flow as an autonomous dynamical system. Details have been provided in KF20. We do not show it here. Here we follow the procedure as given in KF20. Following KF20, we recast Eqn. (9) in the following form

$$\lambda_{12} \left(\frac{dv^2}{dr} \Big|_{r_c} \right)^2 + (\lambda_{11} - \lambda_{22}) \left(\frac{dv^2}{dr} \Big|_{r_c} \right) + \lambda_{21} = 0, \quad (16)$$

where λ s are given by:

$$\left. \begin{aligned} \lambda_{11} &= \frac{dD}{dr} \Big|_{r_c}, & \lambda_{12} &= \frac{dN1}{dv^2} \Big|_{r_c} \\ \lambda_{21} &= \frac{dD}{dr} \Big|_{r_c}, & \lambda_{22} &= \frac{dN1}{dv^2} \Big|_{r_c}, \end{aligned} \right\} \quad (17)$$

which for our case are

$$\left. \begin{aligned} \lambda_{11} &= \frac{2}{nr_c}, \\ \lambda_{12} &= \frac{1}{v_c^2} \left(\frac{1}{2n} + 1 \right), \\ \lambda_{21} &= -\frac{4v_c^2}{r_c^2} \left(\frac{2}{n} + 1 \right) - \frac{8v_c^2(r_c-1)}{r_c^2(r_c-2)^2} + \frac{4(r_c-2)(r_c-4)}{r_c^5}, \\ \lambda_{22} &= \frac{4}{r_c(r_c-2)} - \frac{2}{nr_c} \end{aligned} \right\} \quad (18)$$

We define a Jacobian matrix Λ of the dynamical system at the critical point (r_c, u_c) having λ_{ij} as its elements, given by

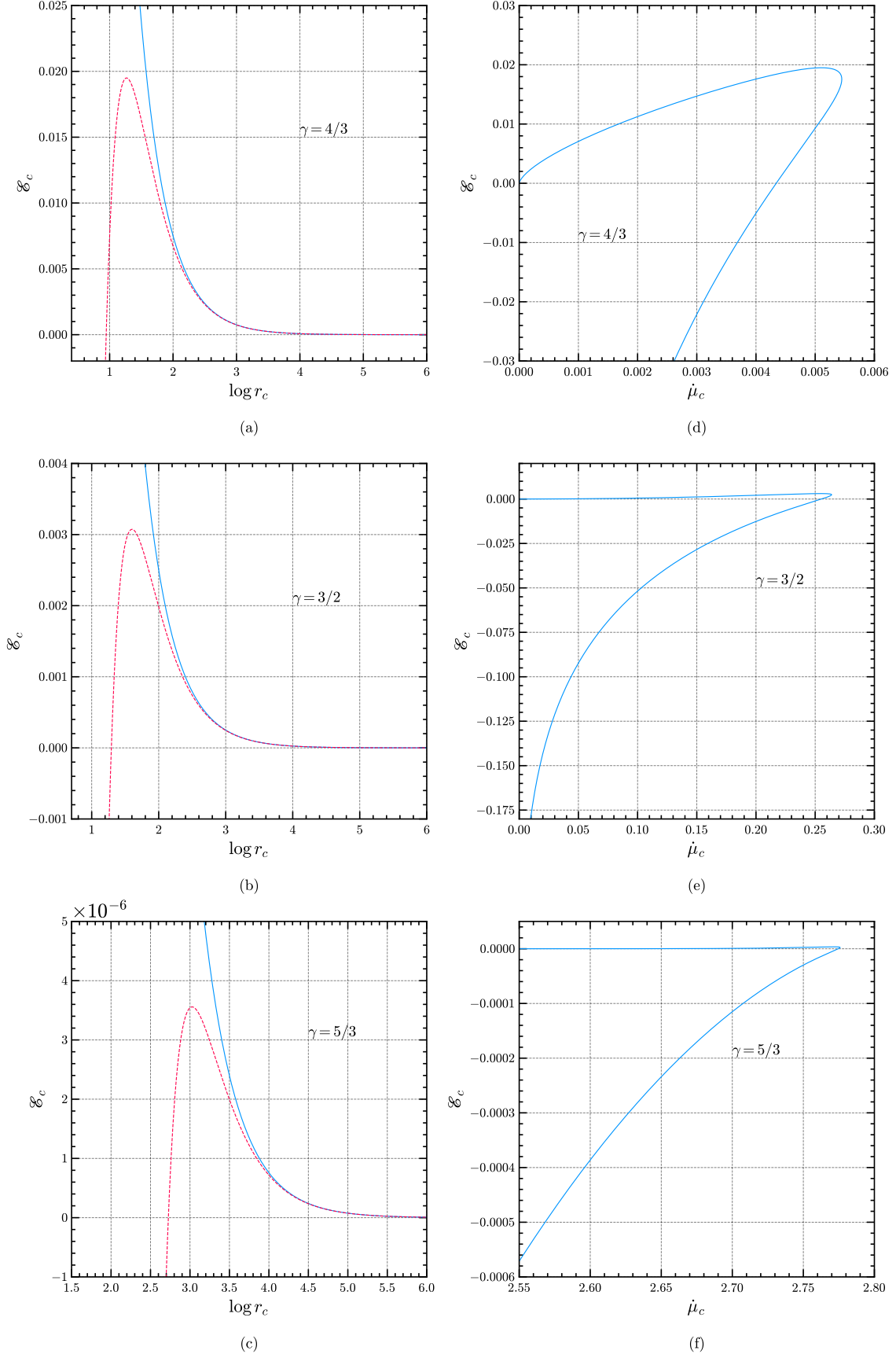


Figure 1: Variation of sonic energy \mathcal{E}_c as functions of sonic location r_c [figures 1(a),(b),(c)] and sonic entropy $\dot{\mathcal{M}}_c$ [figures 1(d),(e),(f)], corresponding to our velocity-dependent potential, for different values of γ . In curves 1(a),(b),(c), solid (blue) line corresponds to classical Bondi case, where as dotted (red) line correspond to velocity-dependent potential. In Figs. 1(d),(e),(f), the curves correspond to velocity-dependent potential. Note that r_c is expressed in units of $r_g = GM_{\text{BH}}/c^2$.

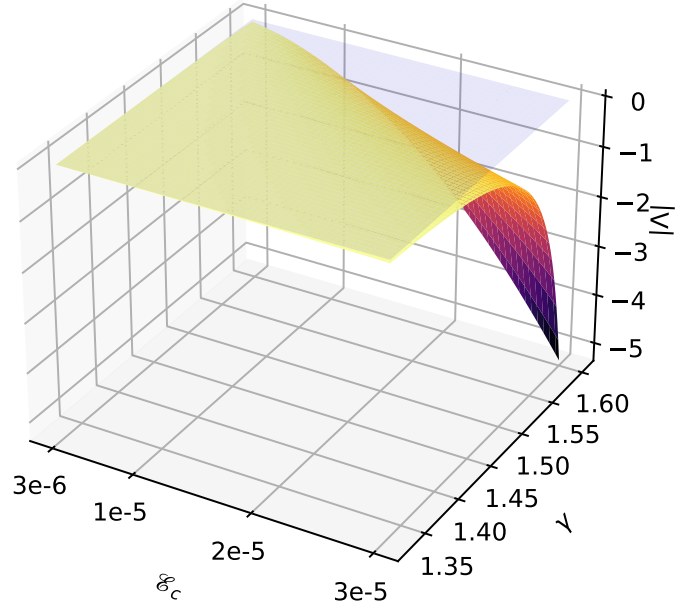
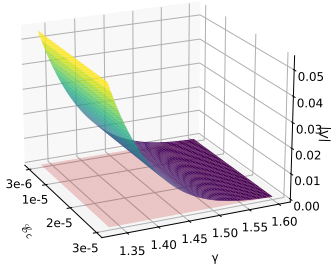
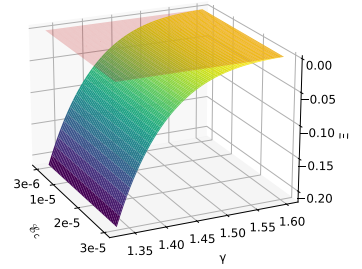


Figure 2: Variation of quantity $|\Lambda|$ (associated with an outer ‘X-type’ sonic point) as a function of parameters \mathcal{E}_c and γ . All values of $|\Lambda|$ are negative for the range of \mathcal{E}_c and γ appropriately chosen here.



(a)



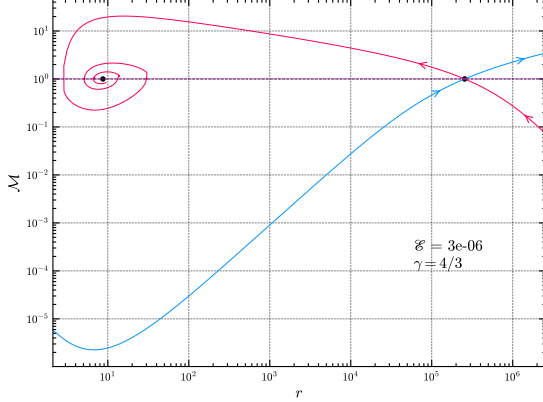
(b)

Figure 3: Variation of quantity $|\Lambda|$ and $\Xi \equiv Tr(\Lambda)^2 - 4|\Lambda|$ (associated with an inner ‘spiral-type’ sonic point) as a function of parameters \mathcal{E}_c and γ . All values of $|\Lambda|$ are positive, whereas all values of quantity Ξ are negative [as shown in figures (3a) and (3b), respectively], for the range of \mathcal{E}_c and γ chosen here.

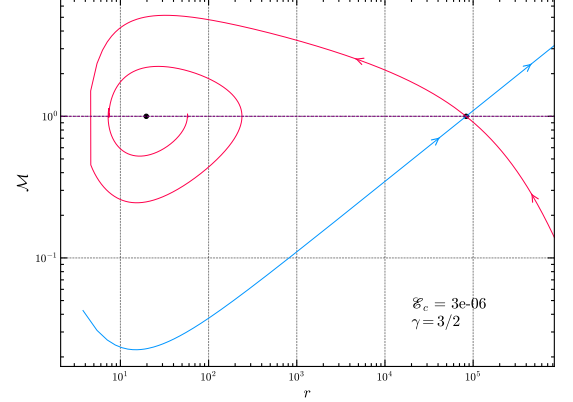
$$\Lambda = \begin{bmatrix} \lambda_{11} & \lambda_{12} \\ \lambda_{21} & \lambda_{22} \end{bmatrix} \quad (19)$$

Table 1: Nature of the critical points

Conditions	Types of critical points
$ \Lambda < 0$	Saddle
$ \Lambda > 0$ and $Tr(\Lambda)^2 - 4 \Lambda \geq 0$	Nodal
$ \Lambda > 0$ and $Tr(\Lambda) = 0$	Centre
$ \Lambda > 0$ and $Tr(\Lambda)^2 - 4 \Lambda \leq 0$	Spiral



(a)



(b)

Figure 4: Variation of Mach number (M) as a function of radial distance (r) representing phase portraits for a few sample cases corresponding to (\mathcal{E}_c, γ) pairs of parameters. The sonic Points are denoted by solid black dots. Outer dot represents outer “X-type” sonic point, whereas the inner dot represent inner “spiral-type” sonic point. Note that r is expressed in units of $r_g = GM_{\text{BH}}/c^2$. The corresponding value of \mathcal{E}_c for which the profiles are generated is given in the respective figures.

where λ'_{ij} are defined in Eqn. (18).

Depending on the values of determinant of $\Lambda(|\Lambda|)$, the trace of $\Lambda[Tr(\Lambda)]$, and the quantity $\Xi \equiv Tr(\Lambda)^2 - 4|\Lambda|$, the nature of critical points of the dynamical system can be determined (KF20). For the sake of completeness, the conditions are tabulated in Table 1 as follows:

The parameter space in our case is defined by sonic energy \mathcal{E}_c and adiabatic constant γ . Figure 2 shows that for all relevant values of \mathcal{E}_c and γ ($4/3 \leq \gamma \leq 5/3$), the corresponding outer sonic points always render $|\Lambda|$ to be negative. On the other hand, corresponding to inner sonic points, for all relevant values of \mathcal{E}_c and γ , $|\Lambda|$ yields positive values, whereas the corresponding quantity $\Xi \equiv Tr(\Lambda)^2 - 4|\Lambda|$ always yields negative values, as depicted in Fig. 3. Moreover, it is clearly seen that for all values of $r_c > 2$, $Tr(\Lambda)$ is always non-zero. Figures 2 and 3 clearly demonstrates that for the range of \mathcal{E}_c and γ appropriately chosen here, outer sonic point is always a ‘saddle-type’ or (‘X-type’), whereas, the inner one is throughout ‘spiral’ in nature.

4. FLUID PROPERTIES AND GLOBAL TOPOLOGICAL PHASE PORTRAITS

The foregoing sections elucidate that the fluid system of our present interest exhibits two sonic points in the flow. Out of two sonic points, the outer sonic point is always “saddle-type” (or “X-type”) through which the sonic transonic occurs, with the flow attaining supersonic speed. Conversely, the inner sonic point is found to be “spiral-type”, which is unphysical, as no stationary solution will traverse through it. To obtain the transonic flow profiles and a family of solutions, one needs to supply the value of \mathcal{E}_c as the flow boundary condition at outer sonic point. For a given value of \mathcal{E}_c , using Eqn. (14), one would then be able to determine the corresponding value of r_c . Subsequently, one could then evaluate the fluid velocity and sound speed at r_c using Eqn. (8). These would then be supplied as additional boundary conditions of the flow to evaluate v and c_s from Eqns. (6) and (7). Employing fourth-order Runge-kutta method, the said equations are then solved, integrating from the outer sonic point inwardly and outwardly, simultaneously.

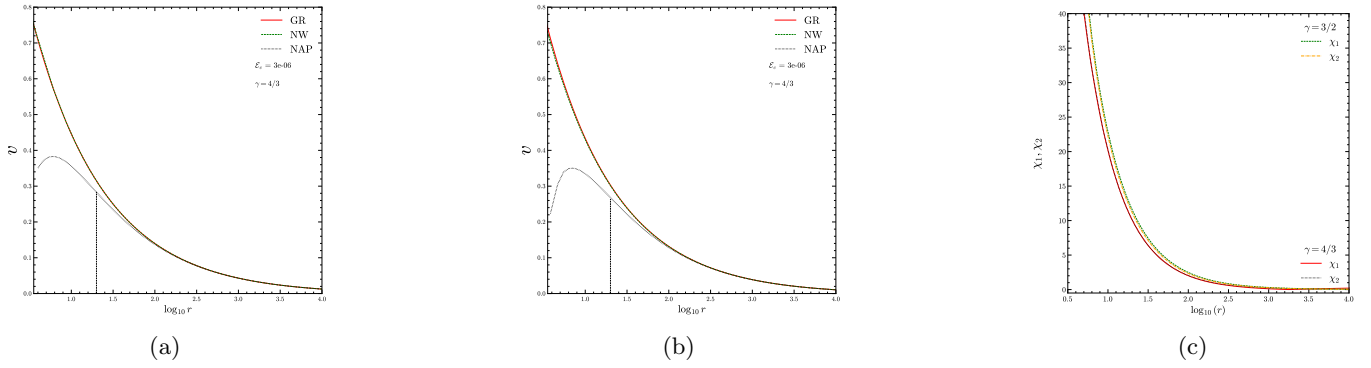


Figure 5: Variation of radial velocity (v) as a function of radial distance (r) for a few sample cases corresponding to (\mathcal{E}_c, γ) pairs of parameters, for the matter passing through the outer sonic point, and a comparison with exact GR and Newtonian Bondi (NW) case. In panels (a) and (b), solid (red) line corresponds to GR case, dashed (green) line corresponds to Newtonian Bondi (NW) case, where as dotted (black) line corresponds to NAP. Vertical lines in both the panels denote the radius, where the deviation from exact relativistic value is approximately 10%. Note that r is expressed in units of $r_g = GM_{\text{BH}}/c^2$. The corresponding value of \mathcal{E}_c for which the profiles are generated is given in the respective figures. In panel (c), we show the relative differences (in percentage) between GR and NAP cases (denoted by quantity χ_1), as well as between Newtonian Bondi (NW) and NAP cases (denoted by quantity χ_2) corresponding to the solutions in panels (a) and (b). In panel (c), solid (green) and dotted (red) lines correspond to χ_1 and χ_2 , respectively, for $\gamma = 4/3$ case, while, dashed (orange) and dotted-dashed (black) lines are similar to solid and dotted lines, respectively, but for $\gamma = 3/2$ case.

In Fig. 4 we show the flow topologies or phase portraits for a few sample cases, in the context of the fluid system of our interest, depicting outer “X-type” sonic point, and inner “spiral-type” sonic point. Here it is important to note that in the context of matter falling into the BH, any physical transonic accretion flow should pass through “X-type” sonic point before entering BH horizon supersonically. Although for our case, one does have an outer “X-type” sonic point, but the solution will not extend supersonically till the horizon, as the inner sonic point appearing to be unphysical (“spiral-type”), will not allow any stationary solution to pass through it. Figure 5(a),(b) shows the variation of radial velocity (v) as a function of radial distance (r), for the matter passing through the outer “X-type” sonic point, and a comparison with the exact GR and Newtonian Bondi cases. Here, relevant for our purpose, in the context of GR solution, we have appropriately chosen the radial component of fluid’s “three-velocity” as measured by a local, stationary (static) observer [see e.g., Shapiro & Teukolsky (1983); Aguayo-Ortiz et al. (2021)], following Mandal et al. (2007), as we make a comparison with respect to fluid velocity in the “Newtonian framework”. This “three-velocity” is related to the radial component of fluid’s “four-velocity (u)” [as used in Michel (1972)] through the following transformation relation (in dimensionless unit) [e.g., Appendix G in Shapiro & Teukolsky (1983)]

$$v = \frac{u}{(1 - 2/r + u^2)^{1/2}}. \quad (20)$$

Also, in terms of this fluid “three-velocity”, it follows that at $r = r_c$, $v = c_s$, that actually justifies calling r_c as sonic radius or sonic point Shapiro & Teukolsky (1983); Aguayo-Ortiz et al. (2021); Mandal et al. (2007). This is similar to the scenario in the “Newtonian framework” (whether in context of Newtonian potential or TR13 NAP). a choice of a comparatively higher value of the energy, or even a lower value, will render an unrealistic value of the ambient temperature.

From the figure, we observe that around ~ 10 Schwarzschild radii, radial velocity v deviates by about $\sim 10\%$ of the exact relativistic value corresponding to $\gamma \sim 4/3$. Similarly for $\gamma \sim 3/2$, a $\sim 10\%$ deviation of v from exact relativistic value occurs around ~ 11 Schwarzschild radii. The actual deviation of radial velocity from classical Bondi case however occurs at around $\sim (40 - 50)$ Schwarzschild radius. For higher values of γ as γ approaches $5/3$, the deviation in v will occur from much larger radii, with higher error in v around 10 Schwarzschild radius. In Fig. 5(c), for more clarity, we show the relative differences between GR and NAP cases, as well as between Newtonian Bondi (NW) and NAP cases, corresponding to the solutions in panels (a) and (b). The (percentage) relative deviation is denoted by the quantity χ ($\chi_1 = \frac{|v_{\text{GR}} - v_{\text{NAP}}|}{v_{\text{GR}}} \times 100$; $\chi_2 = \frac{|v_{\text{NW}} - v_{\text{NAP}}|}{v_{\text{NW}}} \times 100$), as shown in Fig. 5(c). In both figures 4 and 5, we

choose the value of energy $\mathcal{E}_c = 3 \times 10^{-6}$ as boundary condition of the flow. This choice of the value of energy roughly corresponds to a temperature T in the range ($\sim 6 \times 10^6 - 10^7$) K for $4/3 \lesssim \gamma \lesssim 5/3$, a reasonable scenario for the interstellar medium (ISM) at the center of a galaxy [e.g., [Narayan & Fabian \(2011\)](#); [Raychaudhuri et al. \(2018\)](#)]. For a slight increase in the value of energy \mathcal{E}_c , there will be no appreciable change in the radial-limit, mentioned before. On the other hand, for a decrease in \mathcal{E}_c , the deviation in v from that of classical Bondi case will occur from a slightly lesser radius. However, note that, a choice of comparatively higher value of energy, or even a lower value, will render unrealistic value of ambient temperature.

It is interesting to note that, in the context of GR case, at large r , away from the horizon, fluid's "three-velocity (v)" \simeq "four-velocity (u)" [as seen from the Eqn. (20); also see [Shapiro & Teukolsky \(1983\)](#)]. Again at $r \ll r_c$, as the flow moves inward, square of the "four-velocity" " $u^2 \approx 2/r$ " [see e.g., Appendix G in [Shapiro & Teukolsky \(1983\)](#) (Eqn. G.34)], implying that " $v \simeq u$ " [from Eqn. (20)]. Thus in the context of GR case, the solution in terms of radial component of "three-velocity" (that we appropriately used in our study) will remain almost identical to that of solution in terms of 'four-velocity'. We have verified this by actually finding the velocity solution in terms of "four-velocity", employing the above velocity transformation. We do not show it here. Thus, no significant difference would arise in our findings, had radial component of "four-velocity" is instead being used, for comparison.

Here, it is worthy to mention that, had three sonic points (or critical points) appeared in our flow [as being found in advective type accretion flows (see Chakrabarti and collaborators) or in case of Bondi-type flows [e.g., [Raychaudhuri et al. \(2018, 2021\)](#)], and where both inner and outer sonic points being "saddle-types" (or "X-types"), the flow would have possibly passed smoothly through either of the "X-type" sonic points or pass through the inner "X-type" sonic point after encountering a shock, reaching BH horizon supersonically, thereby physically connecting infinity to the horizon. In the next section, we discuss the plausible reasons behind the discrepancy found in our study.

We further compute Bondi mass accretion rate (\dot{M}_B) which can be defined in terms of the transonic quantities of the flow, and compare that with the GR case. In the steady state, corresponding to our NAP, one can write Bondi accretion rate (\dot{M}_B) in the Newtonian framework, given by

$$|\dot{M}_B|_{\text{NAP}} = 4\pi r_c^2 c_{\text{sc}} \rho_c, \quad (21)$$

where ρ_c is the density at the (outer) sonic location. Using the relation $\rho_c = \rho_{\text{out}} \left(\frac{c_{\text{sc}}}{c_{\text{out}}}\right)^{2/(\gamma-1)}$, where ρ_{out} and c_{out} are the corresponding density and sound speed at the outer accretion boundary r_{out} [see §6 in [Raychaudhuri et al. \(2018\)](#)], and using Eqn. (8), one can define $|\dot{M}_B|_{\text{NAP}}$ in terms of only sonic radius (r_c) and outer boundary conditions. Note that, ρ_{out} is effectively the density of the ambient medium. Similarly, for GR case, following [Mandal et al. \(2007\)](#) [see Eqn. (7) in [Mandal et al. \(2007\)](#)], we make use of the appropriate expression for Bondi accretion rate, in terms of fluid's "three-velocity" (see the discussion in the previous paragraphs of this section), given as

$$|\dot{M}_B|_{\text{GR}} = 4\pi r_c^2 v_c \rho_c \sqrt{\frac{1 - 2r_c^{-1}}{1 - v_c^2}}. \quad (22)$$

One can obtain the above expression from Eqn. (8) in [Michel \(1972\)](#) by replacing 'u' through 'v' using Eqn. (20). Here we note that, in the expression of [Mandal et al. \(2007\)](#) [Eqn. (7)], the factor of '2' arising on the right hand side of the numerator of Eqn. (22), is absent, as the authors in their work have expressed radius r in units of $2GM/c^2$, while we in the present article have expressed r in units of GM/c^2 . Using Eqns. (6) and (9) from [Mandal et al. \(2007\)](#), one can express $|\dot{M}_B|_{\text{GR}}$ solely in terms of r_c and outer boundary conditions. For the case of nonrelativistic baryons accreting from ambient medium (e.g., ISM), as usual one can express c_{out} in terms of T_{out} , the temperature of the ambient medium, given through $c_{\text{out}}^2 = \gamma k_B T_{\text{out}} / \mu m_p$, where k_B is the Boltzmann constant, m_p , the usual mass of proton, and $\mu = 0.592$ is the mean molecular weight for the galactic abundance of Hydrogen and Helium with Hydrogen mass fraction $X = 0.75$. One can then estimate the quantity $|\dot{M}_B|_{\text{NAP}} / |\dot{M}_B|_{\text{GR}}$ in terms of respective sonic locations, and ambient temperature T_{out} , given through

$$|\dot{M}_B|_{\text{NAP}} / |\dot{M}_B|_{\text{GR}} = \frac{\left(\frac{1}{2}\right)^{\frac{\gamma+1}{2(\gamma-1)}} r_c^{\frac{3\gamma-5}{2(\gamma-1)}} \left[\frac{(1-2/r_c)^3}{(1-1/r_c)}\right]^{\frac{\gamma+1}{2(\gamma-1)}} \Bigg|_{\text{NAP}}}{r_c^2 \left(\frac{1}{4r_c-1}\right)^{\frac{\gamma+1}{2(\gamma-1)}} \left[\frac{1-2r_c^{-1}}{1-(4r_c-1)^{-1}}\right]^{1/2} \left[\frac{\gamma-1-1.794 \times 10^{-13} \gamma T_{\text{out}}}{\gamma-1-(4r_c-1)^{-1}}\right]^{\frac{1}{\gamma-1}} \Bigg|_{\text{GR}}}. \quad (23)$$

Here, r_c in the numerator of Eqn. (23) corresponds to (outer) sonic location for NAP, whereas in the denominator it corresponds to GR case.

For any realistic value of the temperature of ambient medium T_{out} , the term $1.794 \times 10^{-13} \gamma T_{\text{out}}$ in the denominator of Eqn. (23) is much less than the preceding term $\gamma - 1$, and hence can be neglected. It is being found that corresponding to different values of γ , the quantity $|\dot{M}_B|_{\text{NAP}}/|\dot{M}_B|_{\text{GR}}$, i.e., the ratio of Bondi accretion rate corresponding to NAP to that corresponding to GR case, is almost equal to 1.

5. DISCUSSION AND REMARKS

The advantage of the velocity-dependent NAPs is that they can accurately describe the relativistic features of corresponding spacetime geometries, including classical predictable GR effects (see for e.g., Ghosh et al. (2016)). This is unlike the case for existing PNPs which are primarily emphasized to reproduce the innermost stable and bound circular orbits of particle motion. Newtonian analogous constructs, on the other hand, are done in a manner intended to correctly reproduce geodesic equations of motion of the parent metric. The corresponding velocity-dependent potentials are, thus, more accurate representations of corresponding spacetime geometries in analogous Newtonian framework, which are uniquely defined. In the context of astrophysical phenomena, where one primarily deals with orbital trajectories or dynamics of particle orbits, like orbital precession, chaotic dynamics of orbits, N-body dynamics, or in the context of tidal disruption of stars by massive BHs, these velocity-dependent NAPs are extremely useful, and in few cases had already been employed (e.g., TR13; Bonnerot et al. (2016)). One of the primary aims of the Newtonian analogous constructs is to accurately study complex relativistic accretion phenomena around BHs/compact objects in Newtonian framework, bypassing GR-hydrodynamics (GRHDs)/GR-magnetohydrodynamics (GRMHDs). It is thus worthwhile to examine, how far one can make use of this formalism in hydrodynamical accretion studies within the framework of standard Newtonian hydrodynamics. The NAP modeled by TR13, under the low-energy limit condition for Schwarzschild spacetime, has been applied to the standard geometrically thin accretion disk and accretion infall of non-interacting particles on to a Schwarzschild black hole, and is found to be in good agreement with the exact relativistic solutions.

In this article, as a further application, we seek to explore the extent to which TR13 NAP could describe a transonic radial/quasi-radial type (hydrodynamical) accretion flow in Schwarzschild spacetime, i.e., Bondi-type hydrodynamical spherical accretion within the framework of standard Newtonian hydrodynamics, by conducting an actual hydrodynamical study of accretion flow dynamics. We find that the fluid system of our present interest shows a deviation from classical Bondi scenario from a relatively large outer radii, with deviation in radial velocity v being $\sim 10\%$ of the exact relativistic value around 10 Schwarzschild radius, corresponding to $4/3 \lesssim \gamma \lesssim 3/2$, for appropriate boundary condition (as depicted in Fig. 5). For more higher values of γ as γ approaches $5/3$, the error in u will be higher. Interestingly, as the flow moves inward, a significant departure from classical Bondi solution occurs; instead of obtaining single ‘‘saddle-type’’ sonic transition in the flow (what is being expected in case of an inviscid spherical accretion flow), two sonic points emerge, with the inner one being an (unphysical) ‘‘spiral-type’’, and outer being usual ‘‘saddle-type’’ (or ‘‘X-type’’) sonic point. This indicates that, although the matter will pass through the outer ‘‘X-type’’ point, with the flow attaining supersonic speed, however, the solution will not extend supersonically till the BH horizon, as the inner ‘‘spiral-type’’ sonic point will not allow any stationary solution to pass through it. The position of the outer sonic point, although matches closely to that of the sonic point corresponding to classical Bondi case, or for that matter, GR Bondi case. We estimated the Bondi mass accretion rate corresponding to the TR13 NAP, which is found to be almost identical to that of the GR case.

One can raise a very pertinent point: why does a transonic radial or quasi-radial hydrodynamical accretion flow towards a BH in the presence of velocity-dependent TR13 like NAP, within the standard Newtonian hydrodynamical framework, shows significant departure from the classical Bondi solution, even though such NAP can accurately capture most relativistic features of Schwarzschild spacetime, as well as describe geometrically thin accretion disks, and reproduce the exact relativistic solutions for particle streamlines much better than existing PNPs?. A deeper look into this issue is warranted. Newtonian analogs of corresponding spacetime geometries have been constructed relative to distant stationary observers. In the GR framework, from the point of view of a distant stationary observer, matter will never appear to reach the BH horizon in the Schwarzschild spacetime. Our findings in this regard, that no transonic accretion flow solution is allowed connecting infinity to the BH horizon, appears to be consistent with the GR description. To have a scenario of transonic accretion flow to the horizon, as in GR, it is important to formulate the problem in the perspective of a local stationary observer. Here one can raise a relevant question—whether it would

be correct to use the velocity-dependent NAP along with nonmodified Newtonian hydrodynamics. In this context, [Witzany & Lämmerzahl \(2017\)](#) previously endeavored to address this aspect (although without undertaking any actual hydrodynamical study) in the language of “time reparameterization” (related to lab frame time and proper time). The authors highlighted the need for modification of the usual (standard) Newtonian fluid equations to effectively implement such a velocity-dependent potential in the Newtonian framework. They concluded that a naive implementation of the corresponding velocity-dependent potential or force term into nonmodified Newtonian hydrodynamics would be erroneous and “could lead to pathological behavior of the fluid near the BH horizon.” In their study, [Witzany & Lämmerzahl \(2017\)](#) attempted to develop a modified hydrodynamical formalism to implement such velocity-dependent potential, albeit through an ad hoc approach, in the framework of so-called “time reparameterization.” Nonetheless, it would be important to note that these aspects related to a “distant stationary observer,” or so-called “time reparameterization,” will, perhaps, be more relevant very close to the BH horizon.

A more pertinent issue in this regard is the following: The relativistic Euler equation involves the pressure gradient term coupled with the metric tensor and fluid velocity [Shapiro & Teukolsky \(1983\)](#). In the non-relativistic limit (nrl) (i.e., for $v^2/c^2 \ll 1$ and $2r_g/r \ll 1$), the GR Euler equation exactly reduces to the original (Newtonian) Euler equation. On the other hand, near the BH horizon, $v^2 \sim \frac{2}{r}$, and thus the pressure gradient term of the GR Euler equation effectively reduces to the corresponding term in the standard (Newtonian) Euler equation. Hence, the Newtonian Bondi solutions remain consistent with the corresponding GR results. In contrast, the Euler-type equation in the presence of velocity-dependent TR13 NAP in the standard Newtonian hydrodynamical framework comprises of separate terms (without any coupling to the pressure gradient) for fluid velocity and mass, without having any offsetting terms [see Eqn. (5)]. Thus the Euler-type equation in the presence of velocity-dependent TR13 NAP (that has been derived directly from spacetime metric), in the framework of standard Newtonian hydrodynamics, does not appear to remain consistent with the corresponding GR hydrodynamics, regardless of the fluid’s energy. This might be the primary reason behind the discrepancy found in our study.

Our study suggests that a (modified) hydrodynamical formalism is needed to effectively implement such a velocity-dependent NAP to describe transonic spherical or quasi-spherical accretion flows onto a BH, as well as in other similar studies. This (modified) formalism should align with the spirit of TR13 like NAP, while remaining consistent with relativistic hydrodynamics. A modified hydrodynamical or magnetohydrodynamical framework consistent with such a velocity-dependent potential would be extremely useful in the context of relativistic accretion flow studies, which could then essentially circumvent GRHD or GRMHD equations. This is a thorough exercise that we endeavor to pursue in the near future. Ideally, any proper hydrodynamical framework should be developed starting from a kinetic approach. In the context of our velocity-dependent potential, whether such a framework could be consistently developed requires thorough examination. We leave this as an exercise for future work

ACKNOWLEDGMENTS

The authors are thankful to the anonymous reviewer for his/her insightful questions and critical comments that helped us to improve the manuscript. Shubhrangshu Ghosh (SG) is grateful to Harish-Chandra Research Institute (HRI) for their hospitality, where the main part of the present work was carried out. SG acknowledge IUCAA, Pune, for their support through the ‘Visiting Associateship Program’.

REFERENCES

- | | |
|--|---|
| Abramowicz M., Czerny B., Lasota J., Szuszkiewicz E., 1988, <i>Astrophysical Journal</i> , 332, 646. | Bhattacharya D., Ghosh S., Mukhopadhyay B., 2010, <i>The Astrophysical Journal</i> , 713, 105 |
| Aguayo-Ortiz A., Tejada E., Sarbach O., López-Cámara D., 2021, <i>Monthly Notices of the Royal Astronomical Society</i> , 504, 5039. | Bondi H., 1952, <i>Monthly Notices of the Royal Astronomical Society</i> , 112, 195. |
| Bauer A. M., Cárdenas-Avenidaño A., Gammie C. F., Yunes N., 2022, <i>The Astrophysical Journal</i> , 925, 119. | Bonnerot C., Rossi E. M., Lodato G., Price D. J., 2016, <i>Monthly Notices of the Royal Astronomical Society</i> , 455, 2253. |
| Benson A. J., Babul A., 2009, <i>Monthly Notices of the Royal Astronomical Society</i> , 397, 1302. | Bu D.-F., Yuan F., Gan Z.-M., Yang X.-H., 2016, <i>The Astrophysical Journal</i> , 823, 90. |

- Chakrabarti S. K., 1989, *The Astrophysical Journal*, 347, 365.
- Chakrabarti S. K., 1990, *Theory of transonic astrophysical flows*, World Scientific.
- Chakrabarti S. K., 1996, *The Astrophysical Journal*, 464, 664.
- Chakrabarti S., Titarchuk L. G., 1995, *The Astrophysical Journal*, 455, 623.
- Chan C.-k., Psaltis D., Özel F., 2005, *The Astrophysical Journal*, 628, 353.
- Chang K., Ostriker J., 1985, *Astrophysical Journal*, 288, 428.
- Ciotti L., Pellegrini S., 2017, *The Astrophysical Journal*, 848, 29.
- Das T. K., 2002a, *Monthly Notices of the Royal Astronomical Society*, 330, 563.
- Das T. K., 2002b, *The Astrophysical Journal*, 577, 880.
- Das T. K., Sarkar A., 2001, *Astronomy & Astrophysics*, 374, 1150.
- Dihingia I. K., Das S., Prabhakar G., Mandal S., 2020, *Monthly Notices of the Royal Astronomical Society*, 496, 3043.
- Flammang R., 1982, *Monthly Notices of the Royal Astronomical Society*, 199, 833.
- Friedman Y., Scarr T., 2019, in *Journal of Physics: Conference Series.*, 1239, 012011.
- Friedman Y., Scarr T., Steiner J., 2019, *International Journal of Geometric Methods in Modern Physics*, 16, 1950015.
- Fukue J., 1987, *Publications of the Astronomical Society of Japan*, 39, 309.
- Ghosh S., Banik P., 2015, *International Journal of Modern Physics D*, 24, 1550084.
- Ghosh S., Mukhopadhyay B., 2007, *The Astrophysical Journal*, 667, 367.
- Ghosh S., Sarkar T., Bhadra A., 2014, *Monthly Notices of the Royal Astronomical Society*, 445, 4460.
- Ghosh S., Sarkar T., Bhadra A., 2015, *Physical Review D*, 92, 083010.
- Ghosh S., Sarkar T., Bhadra A., 2016, *The Astrophysical Journal*, 828, 6.
- Hawley J. F., Balbus S. A., 2002, *The Astrophysical Journal*, 573, 738.
- Hawley J. F., Krolik J. H., 2002, *The Astrophysical Journal*, 566, 164.
- Igumenshchev I. V., 2008, *The Astrophysical Journal*, 677, 317.
- Igumenshchev I. V., Narayan R., Abramowicz M. A., 2003, *The Astrophysical Journal*, 592, 1042.
- John A. J., Stevens C. Z., 2019, *The European Physical Journal C*, 79, 962.
- Jordan D., Smith P., 2007, *Nonlinear ordinary differential equations: an introduction for scientists and engineers*, OUP Oxford.
- Kalita S., Mukhopadhyay B., 2019, *The European Physical Journal C*, 79, 877.
- Kato S., Fukue J., 2020, *Fundamentals of Astrophysical Fluid Dynamics*, Springer; KF20
- Korol V., Ciotti L., Pellegrini S., 2016, *Monthly Notices of the Royal Astronomical Society*, 460, 1188.
- Lipunov V., Gorbovskoy E., 2007, *The Astrophysical Journal*, 665, L97.
- Lu J.-F., Yu K. N., Yuan F., Young E. C. M., 1997, *Astrophysical Letters and Communications*, 35, 389L.
- Mancino A., Ciotti L., Pellegrini S., 2022, *Monthly Notices of the Royal Astronomical Society*, 512, 2474.
- Mandal I., Ray A. K., Das T. K., 2007, *Monthly Notices of the Royal Astronomical Society*, 378, 1400.
- Matsumoto R., Kato S., Fukue J., Okazaki A. T., 1984, *Publications of Astronomical Society of Japan*, 36, 71.
- Michel F. C., 1972, *Astrophysics and Space Science*, 15, 153.
- Mondal T., Mukhopadhyay B., 2019, *Monthly Notices of the Royal Astronomical Society*, 482, L24.
- Mukhopadhyay B., 2002, *The Astrophysical Journal*, 581, 427.
- Mukhopadhyay B., Ghosh S., 2003, *Monthly Notices of the Royal Astronomical Society*, 342, 274.
- Narayan R., Fabian A. C., 2011, *Monthly Notices of the Royal Astronomical Society*, 415, 3721.
- Nobili L., Turolla R., 1988, *The Astrophysical Journal*, 333, 248.
- Nobili L., Turolla R., Zampieri L., 1991, *The Astrophysical Journal*, 383, 250
- Ohsuga K., Mineshige S., 2011, *The Astrophysical Journal*, 736, 2.
- Paczynsky B., Wiita P. J., 1980, *Astronomy & Astrophysics*, 88, 23.
- Ramírez-Velasquez J., Sigalotti L. D. G., Gabbasov R., Cruz F., Klapp J., 2018, *Monthly Notices of the Royal Astronomical Society*, 477, 4308.
- Ramírez-Velasquez J., Sigalotti L. D. G., Gabbasov R., Klapp J., Contreras E., 2019, *Astronomy & Astrophysics*, 631, A13.
- Raychaudhuri S., Ghosh S., Joarder P. S., 2018, *Monthly Notices of the Royal Astronomical Society*, 479, 3011.
- Raychaudhuri S., Ghosh S., Joarder P. S., 2021, *Journal of Cosmology and Astroparticle Physics*, 2021, 025.

- Richards C. B., Baumgarte T. W., Shapiro S. L., 2021, Monthly Notices of the Royal Astronomical Society, 502, 3003.
- Sarkar T., Ghosh S., Bhadra A., 2014, Physical Review D, 90, 063008.
- Shafee R., Narayan R., McClintock J. E., 2008, The Astrophysical Journal, 676, 549.
- Shafee R., Narayan R., McClintock J. E., 2008, The Astrophysical Journal, 676, 549.
- Shapiro, S. L., Teukolsky S. A., 1983, Black holes, white dwarfs and neutron stars. The physics of compact objects, Wiley.
- Tejeda E., Mendoza S., Miller J. C., 2012, Monthly Notices of the Royal Astronomical Society, 419, 1431.
- Tejeda E., Rosswog S., 2013, Monthly Notices of the Royal Astronomical Society, 433, 1930; TR13
- Tejeda E., Taylor P. A., Miller J. C., 2013, Monthly Notices of the Royal Astronomical Society, 429, 925.
- Turolla R., Nobili L., 1988, Monthly Notices of the Royal Astronomical Society, 235, 1273.
- Turolla R., Nobili L., 1989, The Astrophysical Journal, 342, 982.
- Witzany V., Lämmerzahl C., 2017, The Astrophysical Journal, 841, 105.
- Yang S., Liu C., Zhu T., Zhao L., Wu Q., Yang K., Jamil M., 2021, Chinese Physics C, 45, 015102.
- Yuan F., Narayan R., 2014, Annual Review of Astronomy and Astrophysics, 52, 529.